GABPβ1. The fifth cDNA clone was approximately 1.4 kb and differed from the other four at its 3′ end; this cDNA clone encoded GABPβ2. Four additional cDNA clones corresponding to GABPβ2 were subsequently identified.
9. C. C. Thompson, T. A. Brown, S. L. McKnight, *Science* **253**, 762 (1991).
10. D. K. Watson *et al.*, *Proc. Natl. Acad. Sci. U.S.A.* **85**, 7862 (1988).
11. C. V. Gunther, J. A. Nye, R. S. Bryner, B. J. Graves, *Genes Dev.* **4**, 667 (1990).
12. M. Klemsz, S. R. McKercher, A. Celada, C. Van Beveren, R. A. Maki, *Cell* **61**, 113 (1990); M. G. Goebl, *ibid.*, p. 116.
13. L. D. Urness and C. S. Thummel, *ibid.* **63**, 47 (1990).
14. F. D. Karim *et al.*, *Genes Dev.* **4**, 1451 (1990).
15. K. A. Wharton, K. M. Johansen, T. Xu, S. Artavanis-Tsakonas, *Cell* **43**, 567 (1985); I. Greenwald, *ibid.*, p. 583.
16. J. Yochem, K. Weston, I. Greenwald, *Nature* **335**, 547 (1988).
17. J. Yochem and I. Greenwald, *Cell* **58**, 553 (1989); J. Austin and J. Kimble, *ibid.*, p. 565.
18. L. Breeden and K. Nasmyth, *Nature* **329**, 651 (1987).
19. S. E. Lux, K. M. John, V. Bennett, *ibid.* **344**, 36 (1990).
20. S. Gillard, D. Spehner, R. Drillien, A. Kirn, *Proc. Natl. Acad. Sci. U.S.A.* **83**, 5573 (1986).
21. M. Kieran *et al.*, *Cell* **62**, 1007 (1990); V. Bours, J. Vallalobos, P. R. Burd, K. Kelly, U. Siebernlist, *Nature* **348**, 76 (1990).
22. K. L. Stone, M. B. LoPresti, K. R. Williams, *Laboratory Methodology in Biochemistry*, C. Fini, A. Floridi, V. Finelli, Eds. (CRC Press, Boca Raton, FL, 1991).
23. Tryptic peptides were sequenced on an Applied Biosystems 477-A protein sequencer with the standard cycle described by the manufacturer.
24. F. Sanger, S. Nicklen, A. R. Coulson, *Proc. Natl. Acad. Sci. U.S.A.* **74**, 5463 (1977). The complete nucleotide sequences of GABPα, GABPβ1, and GABPβ2 were determined on both DNA strands with deleted templates or synthetic oligonucleotide primers. Deletions were made with exonuclease III (Pharmacia) under conditions specified by the manufacturer. The sequences for GABPβ1 and GABPβ2 were identical up to nucleotide 1130 except for a three-nucleotide insertion (GTA) at position 828 of GABPβ1. Sequencing of four other independent isolates of GABPβ1 was identical to GABPβ2 at this site.
25. J. M. Chirgwin *et al.*, *Biochemistry* **18**, 5294 (1979).
26. P. Chomczynski and N. Sacchi, *Anal. Biochem.* **162**, 156 (1987).
27. P. A. Krieg and D. A. Melton, *Nucleic Acids Res.* **12**, 7057 (1984). Plasmids with cDNAs inserted in the Eco RI and Xho I sites of Bluescript (Stratagene) were linearized with Asp718 and transcribed with T3 RNA polymerase to generate sense strand RNA. RNAs were used to program rabbit reticulocyte lysates under conditions specified by the manufacturer (Promega).
28. M. M. Garner and A. Revzin, *Nucleic Acids Res.* **9**, 3047 (1981); M. Fried and D. M. Crothers, *ibid.*, p. 6505. For DNA binding assays, samples containing in vitro translated protein were incubated in 25 mM tris, pH 8.0, 10% glycerol, 50 mM KCl, 3 mM $MgCl_2$, 0.5 mM EDTA, 1 mM dithiothreitol, and poly(dI·dC) (50 μg/ml) on ice for 10 min, then probe was added and incubation was continued at room temperature for 10 min. The probe was a 180-bp Nco I–Sal I fragment excised from the HSV1 ICP4 promoter. The fragment was labeled by fill-in with the Klenow fragment of DNA polymerase I in the presence of ^{32}P-labeled dCTP. Protein-DNA complexes were subjected to electrophoresis on 5% (30:1) polyacrylamide gels in 0.5× TBE buffer.
29. E. S. P. Reddy, V. N. Rao, T. S. Papas, *Proc. Natl. Acad. Sci. U.S.A.* **84**, 6131 (1987).
30. V. N. Rao *et al.*, *Science* **244**, 66 (1989).
31. K. C. Burtis, C. S. Thummel, C. W. Jones, F. D. Karim, D. S. Hogness, *Cell* **61**, 85 (1990).
32. S. J. Aves, B. Durkacz, A. Carr, P. Nurse, *EMBO J.* **4**, 457 (1985).
33. B. J. Andrews and I. Herskowitz, *Nature* **342**, 830 (1989).
34. A. M. Spence, A. Coulson, J. Hodgkin, *Cell* **60**, 981 (1990).
35. H. Ohno, G. Takimoto, T. W. McKeithan, *ibid.*, p. 991.
36. We thank Z. Cao and S.-J. Lee for providing cDNA libraries; S.-J. Lee for many helpful suggestions; P. Okkema for helpful discussions; J. Montoya and R. Truong for help in the preparation of rat liver nuclear extracts; and B. Kingsbury for expert technical assistance. Supported in part by a fellowship from the Leukemia Society (K.L.), the Jane Coffin Childs Fund for Medical Research (C.C.T.), the Howard Hughes Medical Institute, and the Carnegie Institution of Washington.

3 June 1991; accepted 5 July 1991

Design and Synthesis of a Mimetic from an Antibody Complementarity-Determining Region

HORACIO URI SARAGOVI, DENNIS FITZPATRICK, APICHAYA RAKTABUTR, HIROSHI NAKANISHI, MICHAEL KAHN, MARK I. GREENE*

A technique for producing non-peptide compounds (mimetics) of designed specificities was developed that permitted the synthesis of a conformationally restricted molecule that mimicked the binding and functional properties of monoclonal antibody (MAb) 87.92.6, which recognizes the reovirus type 3 cellular receptor. Binding of either MAb 87.92.6, peptide analogs, or 87.1-mimetic to the cellular receptor inhibited cellular proliferation. The mimetic was a synthetic β-loop structure that mimics the second complementarity-determining region of the MAb. These studies may lead to strategies for the synthetic design of antibody complementarity regions, ligands, and other pharmacologically active agents that are water soluble, resistant to proteolysis, and nonimmunogenic.

ANTIBODIES USE THE COMPLEMENTARITY-determining regions of their hypervariable domains to bind antigens with high affinity and specificity. Synthetic peptides derived from complementarity-determining region (CDR) sequences have properties similar to the intact antibody (*1*). These peptides can inhibit idiotype–anti-idiotype interactions, bind specific antigens, interact with cellular receptors, and stimulate biological processes. For example, MAb 87.92.6 binds to the cell surface receptor for reovirus type 3 (Reo3R). Cyclic peptide analogs derived from the second CDR of MAb 87.92.6 bind with higher affinity to the Reo3R than the corresponding linear peptide analogs do (*2*). However, because of their proteinaceous nature, the peptide analogs tend to be water insoluble, are highly immunogenic, do not readily cross the blood-brain barrier, can adopt various conformations, and are subject to proteolysis (*2*). The usefulness of peptide analogs in vivo is therefore limited.

To synthesize organic compounds with biological activity and without the limitations of peptides, we first determined the relevant contact residues and conformation involved in MAb 87.92.6 binding. Then we developed a method for the synthesis of molecules with that conformation. Computer modeling of the structure of active and inactive cyclic peptide analogs of the second CDR of 87.92.6 allowed the elucidation of charged amino acid residues that were accessible and relevant in binding to the Reo3R (*2–4*). An approach to synthesize conformationally restricted cyclic organic peptides was developed (Fig. 1) (*5, 6*), and we used this strategy to produce a small organic molecule that contains the deduced relevant contact residues from the second CDR of MAb 87.92.6. This compound structurally mimics the 87.92.6 second CDR, and the technique has allowed the first synthesis of a β loop with the structural properties of an antibody. This organically synthesized structure is named the 87.1-mimetic and has a formula mass of 624 g/mol. The 87.1-mimetic is water-soluble and conformationally restricted. Because of its synthetic nature and size, it is resistant to protease activity and should be nonimmunogenic. Furthermore, the mimetic is expected to be permeable to the blood-brain barrier because of its solubility and small size.

To determine whether the 87.1-mimetic has the binding and functional properties of MAb 87.92.6, we compared the mimetic to the MAb and to other compounds. We have shown that the mouse immunoglobulin G

H. U. Saragovi and M. I. Greene, Department of Pathology and Laboratory Medicine, University of Pennsylvania School of Medicine, Philadelphia, PA 19104. D. Fitzpatrick, A. Raktabutr, H. Nakanishi, M. Kahn, Department of Chemistry, University of Illinois at Chicago, Chicago, IL 60680.

*To whom correspondence should be addressed.

(IgG) MAb 9BG5 efficiently binds the intact mouse immunoglobulin M (IgM) MAb 87.92.6 with nanomolar affinity or the 17–amino acid peptide analogs VL and VLA5, derived from the second CDR of 87.92.6. MAb 9BG5 also binds the dimeric form of VL, VLSH (*4*), but not the 15–amino acid peptide analog 1S1, derived from the reovirus type 1 σ-1 protein sequence. We tested immobilized 87.1-mimetic for its ability to bind the MAb 9BG5 idiotype in a solid phase radioimmunoassay (RIA) (Fig. 2A). Specific binding of 87.1-mimetic to MAb 9BG5 was observed that was ~14-fold over the negative control (1S1), and both the VLSH and the VLA5 positive control cyclic analog peptides bound MAb 9BG5 (*2*). Because of the small size of the 87.1-mimetic, much of the binding surface is involved in immobilization on the RIA plate and only a small proportion retains activity. We estimate that MAb 9BG5 binding is a function of only ~10% of the total mimetic species applied to the plates, indicating an actual increase in binding of 140-fold over the 1S1 peptide.

We next tested the ability of soluble 87.1-mimetic to bind MAb 9BG5 (Fig. 2B). Incubation of MAb 9BG5 with soluble 87.1-mimetic, but not with 1S1 control, competitively inhibited MAb 9BG5 binding to solid phase (immobilized) VLSH. The competition by the 87.1-mimetic was dose-dependent, but we did not test whether equilibrium was obtained. An estimated 70- to 700-fold molar excess of 87.1-mimetic over MAb 9BG5 was required for an inhibition of binding to VLSH, which ranged from ~20% to ~50%, respectively. Taken together, these results indicate that the 87.1-mimetic binds to MAb 9BG5 both in a solid phase (Fig. 2A) and in a liquid phase (Fig. 2B) and mimics the binding specificities of MAb 87.92.6.

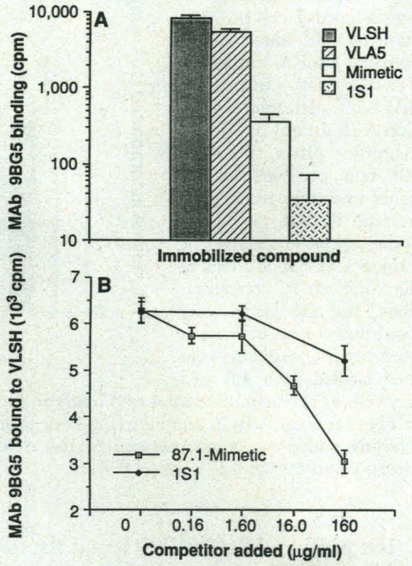

Fig. 2. Binding of 87.1-mimetic to MAb 9BG5. (**A**) MAb 9BG5 binding to immobilized 87.1-mimetic. Each indicated peptide (mimetic) (2.5 μg) in 50 μl of double-distilled water was coupled to polypropylene microtiter plates by evaporation overnight at 37°C. The unreacted sites on the plates were blocked by three 10-min washes in binding buffer (Hanks balanced salt solution, 1.5% bovine serum albumin, and 0.005% sodium azide) and then incubated with 5 μg of protein A–purified MAb 9BG5 in 50 μl of binding buffer for 2 hours at room temperature. After three washes with binding buffer, we added 0.05 μCi (~70,000 cpm per well) of ^{125}I-labeled goat antibody to mouse IgG in 50 μl of binding buffer, incubated the reaction for 40 min at room temperature, and then washed the wells three times with binding buffer. The bound complexes were eluted from the plates by a 3-min wash with double-distilled water containing 1.5% SDS and were counted in a gamma counter. The average background counts per minute of plates without peptides or with isotype-matched irrelevant MAb was 101 cpm and was subtracted from the data shown (n = 11). (**B**) 87.1-mimetic inhibits MAb 9BG5 from binding to solid-phase VLSH. The method was as in (A), except that MAb 9BG5 was incubated for 2 hours at room temperature with or without increasing concentrations of the 87.1-mimetic or 1S1 control before the binding assay. MAb 9BG5 was then tested for its ability to bind VLSH immobilized on RIA plates (n = 4).

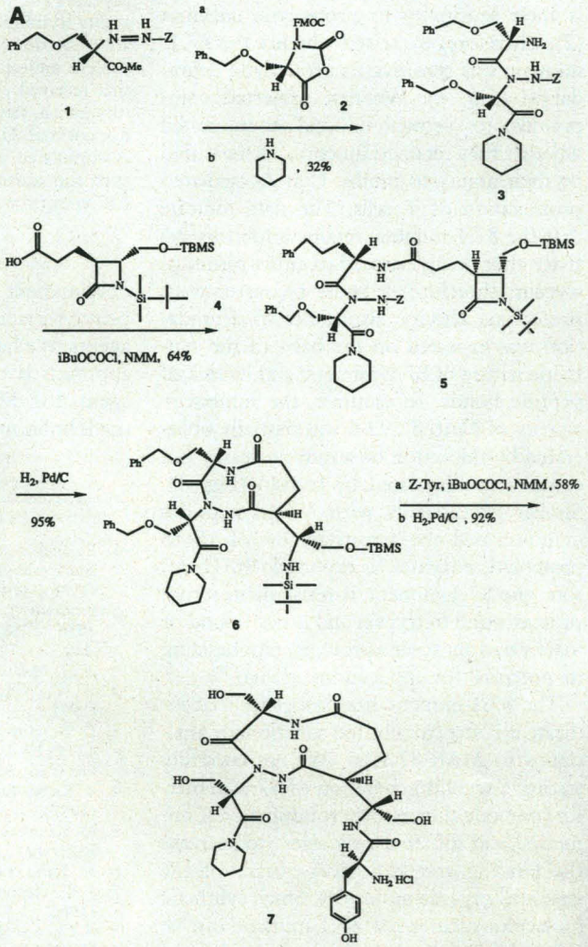

Fig. 1. Synthesis and structure of the 87.1-mimetic. (**A**) Summary of the synthetic pathway for the cyclic organic 87.1-mimetic. The synthesis began with 0.4 mM of an *N*-carbobenzoxy-serine derivative **1** that was dissolved in 5 ml of anhydrous tetrahydrofuran (THF) (*10*). During the coupling of **1** with **2**, the fluoren-9-ylmethoxycarbonyl (FMOC) protected the *N*-carboxyl-anhydride derivative of benzylserine (*11*), and the subsequent deprotection with piperidine yielded the amino amide **3**. Mixed-anhydride coupling with 1.0 mM azetidinone **4** in THF (*12*) yielded the cyclization precursor **5**. Reductive deprotection of the hydrazino group rapidly effected cyclization to the ten-membered ring compound **6** (*13*). Completion of the synthesis was effected by mixed anhydride coupling with *N*-carbobenzoxy-tyrosine (Z-Tyr). Deprotection resulted in mimetic **7**, namely the 87.1-mimetic. Yields are provided as percentages under the arrows and are unoptimized. The 87.1-mimetic was purified to homogeneity by reverse-phase (C_{18}) high-performance liquid chromatography. Detailed description of the synthetic reactions is available from the authors upon request. Z, benzyloxycarbonyl; Ph, phenyl; iBuOCOCl, isobutyl chloroformate; and NMM, *N*-methylmorpholine. (**B**) Space-filling model of the 87.1-mimetic. This model is based on the nuclear magnetic resonance (NMR) coordinates of the 87.1-mimetic and was produced with the Macromodel program on a Silicon Graphics Workstation. Oxygen atoms are colored red, hydrogen white, carbon green, and nitrogen blue. The mimetic structure was characterized by ^{1}H NMR (400 MHz) and Fast-Atom Bombardment Mass Spectroscopy.

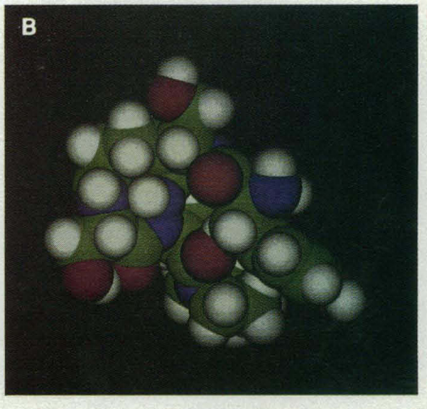

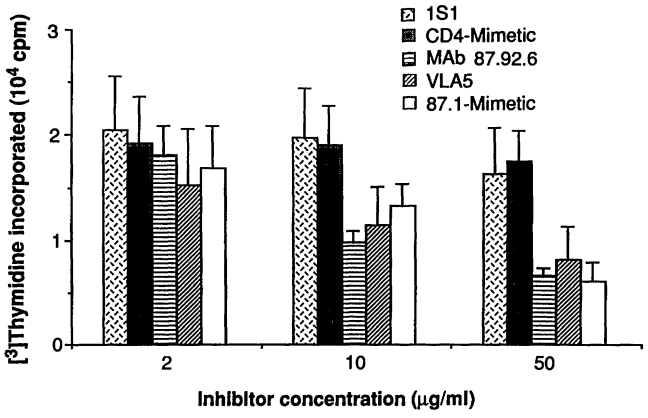

Fig. 3. Inhibition of mitogen-induced T cell proliferation by 87.1-mimetic. We prepared Con A–stimulated T cells by incubating BALB/c splenocytes with Con A (5 μg/ml) in 96-well microtiter plates at 5.0×10^5 cells per well for 24 hours to induce the expression of Reo3R (*9*). Antibodies, peptide analogs, or mimetics were then added at the indicated concentrations, and the plates were incubated for an additional 16 hours. The plates were then labeled with 1.0 μCi per well of [^{3}H]thymidine for 4 to 6 hours and harvested; the incorporated radioactivity was measured in a beta counter with Econofluor (Du Pont Biotechnology Systems) scintillation fluid. Untreated (no inhibitor added) wells incorporated 21,164 ± 5,525 cpm and unstimulated (no Con A added) wells incorporated 699 ± 627 cpm (n = 6).

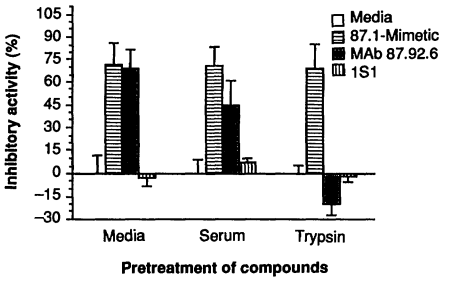

Fig. 4. Resistance of 87.1-mimetic to proteolytic enzymes. Culture media, 87.1-mimetic, MAb 87.92.6, or 1S1 control peptide were each incubated with either culture media, normal rabbit serum (50% v/v, not heat-inactivated), or trypsin–*N*-tosyl-L-phenylalanine chloromethyl ketone (TPCK) (Sigma, 1 mg/ml in phosphate-buffered saline) for 7 hours at 37°C. The mixtures containing trypsin were further treated with a serine protease inhibitor cocktail [soybean trypsin inhibitor (2 mg/ml), TPCK (10 μg/ml), phenylmethylsulfonyl fluoride (10 μg/ml) and leupeptin (10 μg/ml) in culture media] for 1 hour at 37°C. We then tested the mixtures of culture media, 87.1-mimetic (100 μg/ml final concentration), MAb 87.92.6 (50 μg/ml final concentration) or 1S1 peptide (100 μg/ml final concentration) for their ability to inhibit Con A–mediated T cell proliferation as described in Fig. 3. We determined percent inhibition by normalizing to 0% the cells that received culture media pretreated with culture media, serum, or trypsin plus protease inhibitor cocktail. Untreated (no inhibitor added) Con A–stimulated T cells incorporated 8,641 ± 958 cpm and unstimulated (no Con A) cells 720 ± 647 cpm (n = 4).

The peptides VLA5, VLSH, and the intact MAb 87.92.6 interact with the Reo3R. Receptor binding leads to an arrest of mitogen-induced DNA synthesis of T cells (*7*). The 87.1-mimetic inhibited concanavalin A (Con A)–induced T cell proliferation of splenocytes in a dose-dependent fashion, as did the VLA5 peptide and the intact MAb 87.92.6 (Fig. 3). In contrast, the 1S1 peptide analog and a CD4-mimetic (a reverse-turn mimetic derived from residues 41 to 54 of human CD4 with a formula mass of 724 g/mol) had no effect on the mitogenic response. The CD4-mimetic was functional and inhibited binding to soluble viral recombinant gp120 to CD4-expressing cells (*8*). Finally, high doses of the 87.1-mimetic had no effect on the proliferation of EL4 mouse thymoma cells that lack the Reo3R and do not bind MAb 87.92.6, yet high doses inhibited proliferation of R1.1 mouse thymoma cells that express the Reo3R and bind the MAb 87.92.6 (*9*). A representative [^{3}H]thymidine incorporation assay indicated that the 87.1-mimetic inhibited R1.1 cells by 56% and by −5% for EL4 cells. The counts per minute incorporated for 87.1-mimetic–treated (100 μg/ml) or untreated control R1.1 cells were 1057 ± 165 versus 2439 ± 106 and for EL4 cells were 1683 ± 325 versus 1590 ± 169, respectively. (Error limits of ±2 SEM are used throughout the paper.) Collectively these data indicate that the inhibitory effects are mediated through binding to the Reo3R. From three independent experiments (Fig. 3), we extrapolated the concentration of inhibitor required for 50% inhibition of proliferation. The estimated concentration for the intact MAb 87.92.6 was 15 to 20 nM. The VLA5 peptide and the 87.1-mimetic required concentrations of 10 to 20 μM and 55 to 70 μM, respectively, nearly three logarithmic units higher than the intact MAb; this assay compares the activity of a monomeric 87.1-mimetic to a decameric (MAb 87.92.6 IgM) form of the ligand.

A major disadvantage of peptide analogs is their sensitivity to proteolytic enzymes (*2*). Therefore, we tested whether the 87.1-mimetic was sensitive to proteolytic degradation (Fig. 4). We first subjected compounds to proteolysis and then tested whether they retained function, as measured by their ability to inhibit Con A–mediated proliferation of T cells. The data indicate that the 87.1-mimetic retains inhibitory activity after being exposed to either serum or trypsin; therefore, it must be resistant to proteolytic activity. Resistance to degradation was expected on the basis of the synthetic nature of 87.1-mimetic and its lack of peptide bonds. In contrast, the inhibitory activity of MAb 87.92.6 was partially obliterated by the action of serum proteases and completely eliminated by trypsin (Fig. 4). Similar experiments with VLA5 peptides demonstrated the sensitivity of VLA5 to proteolytic enzymes, as expected (*9*). Therefore, the 87.1-mimetic is resistant to serum proteases and to trypsin and is not bound or inactivated by serum proteins, emphasizing its potential for applications in vivo.

The 87.1-mimetic has properties that indicate it is structurally and functionally analogous to MAb 87.92.6. We are currently testing a second generation of 87.1-mimetics (mimetic dimers, heterobifunctional mimetics, and different ring sizes) to increase the binding and biological efficacy of the designed organic molecules. Small synthetic molecules such as the 87.1-mimetic can be tailored to mediate the biological effects of antibodies or other ligands. These mimetics should possess beneficial properties, such as an increased half-life, an ability to cross the blood-brain barrier, and a lack of immunogenicity, and thus should be useful for the development of new pharmaceutical, therapeutic, diagnostic, and receptor-binding agents. We have already established that this approach is useful for developing new reagents for different members of the immunoglobulin multigene family.

REFERENCES AND NOTES

1. R. Taub *et al.*, *J. Biol. Chem.* **264**, 259 (1989); C. Bruck *et al.*, *Proc. Natl. Acad. Sci. U.S.A.* **83**, 6578 (1986); C.-Y. Kang, T. K. Brunck, T. Kieber-Emmons, J. E. Blalock, H. Kohler, *Science* **240**, 1034 (1988); W. V. Williams *et al.*, *Proc. Natl. Acad. Sci. U.S.A.* **86**, 5537 (1989); J. Novotny *et al.*, *J. Mol. Biol.* **189**, 715 (1986).
2. W. V. Williams *et al.*, *J. Biol. Chem.* **266**, 5182 (1991).
3. D. Segal *et al.*, *Proc. Natl. Acad. Sci. U.S.A.* **71**, 4298 (1974); L. Amzel *et al.*, *ibid.*, p. 1427; P. de la Paz *et al.*, *EMBO J.* **5**, 415 (1986).
4. T. Kieber-Emmons *et al.*, *Int. Rev. Immunol.* **2**, 339 (1987).
5. M. Kahn *et al.*, *J. Mol. Recognition* **1**, 75 (1988); M. Kahn *et al.*, *J. Am. Chem. Soc.* **110**, 1638 (1988).
6. M. Kahn *et al.*, in preparation.
7. J. T. Nepom *et al.*, *Surv. Immunol. Res.* **1**, 255 (1982).
8. S. Chen *et al.*, in preparation.
9. H. U. Saragovi, unpublished data.
10. R. V. Hoffmann and H.-O. Kim, *Tetrahedron Lett.* **31**, 2953 (1990).
11. W. D. Fuller *et al.*, *J. Am. Chem. Soc.* **112**, 7414 (1991).
12. Azetidinone can be prepared from commercially available D-aspartic acid dimethyl ester as outlined below.

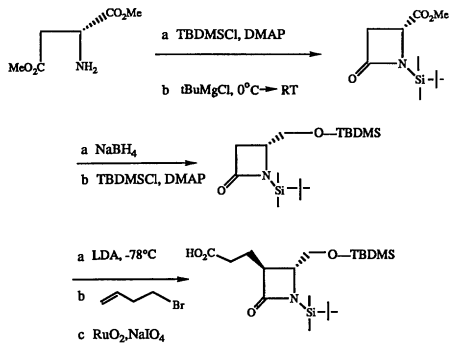

Me, methyl; TBDMSCl, *tert*-butyldimethylsilyl chloride; DMAP, dimethylaminopyridine; tBuMgCl, *tert*-butyl magnesium chloride; RT, room temperature; and LDA, lithium diisopropylamide.

13. H. H. Wassermann, *Aldrichimica Acta* **20**, 63 (1987).

14. Supported by a grant from the National Eye Institute (to M.I.G.) and by an NSF grant (to M.K.). Additional support was from the Lucille P. Markey Charitable Trust (to M.I.G.) and the American Heart Association, Camille and Henry Dreyfus Foundation, and American Cyanamid (to M.K.). We thank W. V. Williams, G. N. Gaulton, and R. A. Chrusciel for helpful discussions and review of this manuscript; W. C. Still (Columbia University, New York) for a copy of Macromodel; and K. Koopferstock for assistance. Coordinates of the 87.1-mimetic structure will be submitted for deposit in the Brookhaven Protein Data Bank.

15 March 1991; accepted 4 June 1991

Photoperiodism and Effects of Indoleamines in a Unicellular Alga, *Gonyaulax polyedra*

IVONNE BALZER AND RÜDIGER HARDELAND

Mediation of photoperiodic effects by indoleamines, especially melatonin, is known in higher vertebrates. A similar mechanism may occur in a unicellular alga, the dinoflagellate *Gonyaulax polyedra*. This organism entered the dormant stage of a cyst upon short-day treatment at lowered temperatures. Interruption of darkness by 2 hours of light prevented cyst formation, even when the overall duration of light was the same as in cyst-inducing short days. When given in a noninducing photoperiod, melatonin and an analog, 5-methoxytryptamine, substances that had previously been shown to occur in *Gonyaulax*, provoked cyst formation. Methoxylated indoleamines may play a role as mediators of darkness in this unicellular, in a similar way as in vertebrates, suggesting a common biochemical basis of photoperiodism.

PHOTOPERIODIC TIME MEASUREMENT has evolved as a means for orientation within the year in organisms phylogenetically as distant as vertebrates, arthropods, and angiosperms. Whether or not a similar physiological basis for photoperiodic mechanisms exists, that can be attributed to the same evolutionary origin, is a matter of discussion.

In vertebrates, information about the relative lengths of photophase and scotophase is mediated by the indoleamine melatonin (*1–4*). However, the occurrence of melatonin is not restricted to these organisms. It exists also in insects, where this substance exhibits a circadian rhythm (*5–7*). In planarians, an effect of melatonin on reproduction has been described (*8*). In the dinoflagellate *Gonyaulax polyedra* we have recently detected two methoxylated indoleamines, melatonin and 5-methoxytryptamine, as well as enzymes involved in their formation, indoleamine *N*-acetyltransferase and hydroxyindole *O*-methyltransferase (*9, 10*). Moreover, melatonin exhibits a daily rhythm of high amplitude, with a nocturnal maximum as high as in vertebrate pineals (about 2.5 ng per milligram of protein) (*11*). We, therefore, tested this organism for a photoperiodic response and for its possible mediation by these indoleamines.

Gonyaulax polyedra was grown at 20°C in a light-dark cycle of 12:12 hours (LD 12:12) (*12*). Photoperiodic experiments were carried out at either 20° or 15°C, under various LD schedules. Light intensity was 400 lux. Cells were transferred to experimental conditions 3 hours after onset of light (circadian time 3 hours); this time point was chosen as the beginning of illumination in the new LD. Melatonin and 5-methoxytryptamine were dissolved directly before use in dimethyl sulfoxide (DMSO), at a concentration of 0.2 M, and then diluted in culture medium to give the desired molarity. DMSO in the molarities used was without effect. Five cultures were used for each data point, and cyst numbers were determined daily.

In the species investigated, photoperiodic responses were unknown. We detected that the cells can, in fact, react by entering a dormant stage. According to morphological criteria, the resting cells are of the type of so-called "thin-walled" or "temporary" cysts (*13*). The process of encystment involves cessation of movement, loss of flagella, retraction from the theca, and formation of a spherical cyst wall. The cyst is finally released from the theca. Cyst formation was quantitatively evaluated by calculating the ratio of cyst to total cell numbers. For definition of the stage of cyst, we used the most unambiguous criterion of a clearly visible cyst wall. Damaged cells were excluded from the evaluation.

At a temperature of 15°C, encystment was strictly photoperiodically controlled (Fig. 1). At a subcritical day length of 11 hours, almost no cyst formation was observed. But a day length of 10 hours or less caused practically all cells to encyst within 4 days. Treatment with a single long dark period sufficed in many experiments to induce cyst formation in up to 20% of cells (Table 1).

A lowered temperature, as compared to normal growing conditions, appears to represent a prerequisite for enabling the cell to respond photoperiodically. At 20°C, cyst formation was negligible even at LD 6:18, whereas the same short day treatment at 15°C led to complete encystment. The inefficiency of short photoperiods at 20°C was supported by extended experiments lasting for several weeks (Table 1).

Photoperiodism cannot be demonstrated solely by comparing effects of long and short days, because the variation of day length is accompanied by changes in the amount of light. This is particularly important in photoautotrophic organisms such as *Gonyaulax*, in which light deficiency could become limiting for cell metabolism. Moreover, encystment has been attributed in dinoflagellates to unfavorable environmental conditions (*13*). Therefore, we carried out experiments in which we interrupted the dark period by

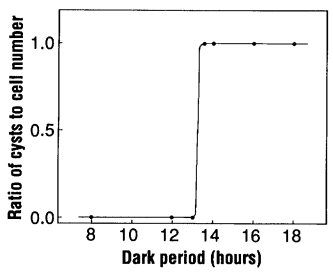

Fig. 1. Cyst induction by short days and decreased temperature. Cultures of mastigote cells were transferred from 20° to 15°C and from LD 12:12 to the experimental LD cycles; the relative number of cysts was determined 4 days after transfer. Experiments were carried out in five cultures with triplicate determinations, but statistical variation was negligible, because cells responded practically in an all-or-none fashion. Ordinate: ratio of cysts to total cell number; abscissa: length of dark period (hours) within an LD cycle of 24 hours.

Zoologisches Institut, Universität Göttingen, Berliner Strasse 28, D-3400 Göttingen, Federal Republic of Germany.